Development, Instrumentation, and Analysis of Recoil through a Riflescope

José Simões [1,2], Eurico Seabra [1], Nuno Dourado [2], Doug Hart [3]

[1] *MEtRICs - Centre for Mechanics and Materials Technologies and Unit of Environmental Biotechnology - School of Engineering, University of Minho, Campus de Azurém, 4800-058 Guimarães, Portugal*
[2] *CMEMS - Center for MicroElectroMechanics Systems - School of Engineering, University of Minho, Campus de Azurém, 4800-058 Guimarães, Portugal*
[3] *MIT - Massachusetts Institute of Technology - Department of Mechanical Engineering, Cambridge, Massachusetts, United States of America*

Abstract

The research and development of new technologies to incorporate in the sport optics field have orientated the design, development, and construction of new riflescopes with state-of-the-art materials, processes, and technology. With each evolution, the riflescope should be evaluated to observe and acquire data on how the riflescope behaves during recoil. For this, the data acquisition and test setup should be easy to maintain, portable, and fast setup addition, measurements should be repeatable and low-cost. A literature review was conducted to check what has been done, what sensors and data acquisition controllers were used, the setup type, and the results. The sensor selection process required numerous specifications to filter the possible sensors for the ideal selection. The main factors and basis for the appointment were weight, G force, frequency, and price. The calculated theoretical max acceleration suffered by the rifle setup is 114g. The sensor also must be easily mounted/unmounted to/from the riflescope body. Furthermore, the sensor should be rigidly fixed not to suffer any unnecessary vibration from the interface and interfere with the measured data. Finally, the data acquisition should be accomplished relatively quickly to measure all the necessary data points. Sensors and accessories from various manufacturers were researched that fit the requirements. However, due to cost limitations, the selected sensor was the ADXL372. The testing setup includes a rifle and riflescope assembly on a stand. The sensor is guided and fixed on the riflescope, and a microcontroller reads and stores the acquired values. As a result, the testing setup is easy to transport and has a quick and repeatable structure. The measured acceleration values can calculate acceleration curves, displacement, velocity, and forces. The setup is ideal as it can be used to monitor the riflescope reaction on each test point, and results can have many uses, such as validating a numerical model FEA simulation. This paper will present and discuss the instrumentation and setup needed to read acceleration values on a riflescope from the firearm recoil and analyze the data for further use and interpretation.

Keywords

Rifle scope, Recoil, accelerometer, MEMS, ICP, Arduino, ADXL372.

1. Introduction

For any data acquisition application, it is critical to dimension the sensor and controller to the application correctly. Otherwise, the setup could be over-dimensioned, meaning it would be more expensive than necessary. Alternatively, it may be under-dimensioned, meaning that the setup will not be able to characterize the application correctly. It is essential to analyze the equipment specifications used in other works for a similar application. A rough calculation may also help to define relative sensor working values.

Using kinematic equations with Newton's second and third laws, it is possible to give a rough estimate of the rifle recoil. For example, solving with projectile and rifle assembly parameters would give a rifle acceleration of 1,119.8 m∕s^2 or 114.1 G.

Although more rifle and bullet variations need to be used in these calculations to verify if this value has drastic changes from one possible setup to another, it is a rough estimate and will be used for the sensor selection. For example, Mathilda Liennard et al. [1] measured a projectile's acceleration directly and performed a simulation of the same setup. This author concluded that the two curves matched quite well. Although in her findings, the projectile reached an acceleration of around 6.5×10^4 G, this value is approximate to the calculated projectile acceleration value of 5.8×10^5 m/s2 or approximately 5.8×10^4 5.8×10^4G used to calculate the rifle recoil.

Elizabeth Brueck [2] also performed various recoil measurements at the stock of a rifle to see if adding a moderator to the rifle would attenuate the felt recoil by the shooter. From this author's ten tests with different rifles and different ammunition, the highest read value was 760 m/s2 or approximately 76 G.

B. Lonzi et al. [3] also measured a rifle's recoil using an accelerometer and a load cell. In the presented work, the maximum recoil force measured was 1241.3 N, i.e., well below our recoil force.

The sensors that make the most sense for the required measurements are accelerometers. The sensors must be lightweight and easily mounted/unmounted to/from the riflescope body. The sensors should be rigidly fixed not to suffer any unnecessary vibration from the interface and interfere with the measured data.

Finally, the data acquisition should be accomplished relatively quickly to measure all the necessary data points. According to other works, it should be at least 200 kHz. Also, from a theoretical max acceleration calculation, the required G value is around 114 Gs, which is almost double the value other researchers have obtained.

There are three different main types of accelerometers. These are piezoelectric, piezoresistive, and capacitive accelerometers.

Piezoelectric accelerometers use a quartz crystal or a lead zirconate titanate (PZT) to produce a small electrical charge proportional to the acceleration disturbance [4–6].These are AC response accelerometers and can be of two types, charge output, and voltage output.

The charge output accelerometers generally require a charge amplifier and a low-noise shielded cable due to their high impedance characteristics. These sensors are considered the most durable due to their ability to tolerate aggressive environmental conditions when hermetically sealed in a welded metal housing. Such conditions include harsh temperatures from -200C to +640C [7].

Conversely, a voltage mode piezoelectric accelerometer includes an onboard charge amplifier to output the voltage. These are also known as ICP types from PCBPIEZOTRONICS. These accelerometers tend to be more sensitive to harsh environments due to their onboard amplifier and have a limited working range for the same reason [7-8].

Piezoresistive accelerometers are in a way similar to a stress gauges. The piezoresistive material changes its resistance when a force is applied. This change in resistance is then converted to an acceleration measurement [4], [9], the output of piezoresistive sensors tends to be sensitive to temperature changes. Therefore, most have an onboard ASIC chip for signal conditioning and temperature compensation. These are also either gas (MEMs) or fluid (strain gauge) damped to prevent sensor resonance and improve dynamic range in high input frequencies. Some can handle frequencies up to 10,000 g making them well-suitable for impulse and impact measurements in automotive or weapons testing [7].

Capacitive accelerometers use MEMs or Micro-Electro-Mechanical systems to operate. MEMS accelerometers are known to be small, lightweight, and relatively cheap [5], [7], [10–12]. Alternatively, they tend to have a poor signal-to-noise ratio (SNR) and a reduced dynamic range.

The maximum range is usually less than 200. These sensors contain an onboard amplifier and are relatively easy to interface with while requiring a stable DC power source [7]. Due to the many works involving MEMs accelerometers, these are the most mature among inertial MEMs [13].

Various manufacturers have been searched for sensors and accessories that fit the requirements, such as PCB Piezotronics [8], Kistler [14]–[16], and DEWESoft [17]. Unfortunately, such sensors, DAQ systems, and accessories do not qualify as a "low-cost system" the end cost would be in the several thousands of dollars range. For a low-cost budget, a MEMs accelerometer would have to be acquired.

As with any input or sensor device, noise is always an issue. Noise sources may include mechanical noise, thermal noise, amplifier noise, sensor-charging reference voltage noise, clock jitter noise, and quantization noise [18-19].

MEMs sensor manufacturers reduce unwanted noise is to add a low-pass or anti-aliasing filter before passing data through the ADC [19]. The ADC may be the most prominent noise contributor to the entire system if not correctly dimensioned by the manufacturer [20]. Leslie Pupo [21] suggests using the Allan Variance method for identifying and characterizing noise in inertial sensors.

Although, in general, low-noise accelerometers have integrated electronics to reduce the distance from the sensor to the amplifier, thus reducing the capacitance and eliminating the noise source [22].

There are numerous ways to reduce noise in accelerometer data. The most common ways include a low pass filter [23], averaging data, and sometimes oversampling and averaging [24]. In any case, it is essential to know how much noise a sensor has. Each sensor has a noise specification described in µg/√Hz on its datasheet. This specification transforms the noise at a given frequency into g terms [25].

In addition, some datasheets have the noise value described in LSB or the least significant bits. These are the number of bits that may have noise, and when subtracted from the sensor's bit resolution, can be used to calculate the minimum detected acceleration (MDA) for the sensor, as shown in the equation 1 [26].

$$MDA = r/2Ne \qquad (1)$$

Where r is the total sensor measurement range, and Ne is the number of effective bits, or total bits minus LSB.

2. Methodology

There are numerous MEMs accelerometers manufacturers available on the market. But most source their ICs from Analog Devices. Table 1 shows a filtered selection of accelerometers available from Analog Devices and their biggest differentiators. The initial filter required that the accelerometers measure at least ±200g and be triaxial. Triaxial accelerometers offer simultaneous measurements in three orthogonal directions enabling the entire movement being suffered by a structure to be analyzed [8], [27].

All table values are for the IC itself except for the cost; this is in reference to the evaluation board.

Table 1

Accelerometer sensors available from Analog Devices

Model	ADXL371 [28]	ADXL372 [29]	ADXL375 [30]
Type	Mems	Mems	Mems
# axis	3	3	3
G rating	±200	±200	±200
Weight [mg]	18	18	30
Dimensions [mm]	3 x 3.25	3 x 3.25	5x 3
ODR (Output data rate) [Hz]	320-5120	400-6400	0.1-3200
Resolution [Bits]	12	12	16
Noise [µg/√Hz]	6.5	4	5
Bandwidth [kHz]	3.2	3.2	1.6
Price [€]	30.72	33.51	38.52

All table values are for the IC itself except for the cost; this is in reference to the evaluation board.

The chosen accelerometer was the ADXL372 due to its higher ODR to read more and higher frequencies. The ADXL372 also comes with an Arduino shield for easy setup and integration. Sample code has also been made available from Analog Devices. The Arduino Uno microcontroller was a good fit since it can communicate easily with the ADXL 372 accelerometer through SPI using the sample code. In addition, the processor was fast enough for the sensor's maximum data output, and gathering all the data through the serial port would be easy. The sensor has a calculated minimum detected acceleration of 1.1 g.

The sample code consists of many adjustable sensor parameters such as ODR, bandwidth, operating mode, wake-up rate, set activity and inactivity threshold and time, and FIFO operation.

Initially, the Arduino was programmed to fetch the accelerometer values one by one and write them each time to the serial monitor. However, this proved insufficient due to the considerable time delay in reading and writing the data. The code was then adjusted to save all the values in local memory and dump all values to the serial monitor simultaneously. This change significantly improved the ODR to the desired values.

The Arduino Uno board could read up to 100 data points for each axis before filling the internal memory. Through trial and error, it was verified that the Arduino UNO's available memory was insufficient to gather all the required data. An upgrade to the Arduino Mega would be necessary.

The Arduino documentation indicates that the Slave Select (SS), also known as the Chip Select (CS), is different for the Arduino UNO and the Arduino MEGA. The CS pins for the Arduino UNO and Arduino MEGA are pins 10 and 53, respectively. Once the shield correctly worked with the Arduino Mega board, it was possible to print 450 data points for each axis.

For attaching the ADXL 372 to the riflescope, a support guide was manufactured and glued precisely onto the riflescope objective with epoxy. The support contains a hole and slot with tight tolerances to position the accelerometer and two screw holes to hold it. So, a couple of calibrated pins were secured to the PCB with epoxy to precise position the accelerometer sensor. This setup facilitates mounting and systematically unmounting the sensor when needed. This setup also allows for more support structures on different riflescope areas and precisely moves the sensor from one support to another and back again to gather more data.

The ADXL372 evaluation board is meant to be placed directly on the Arduino shield. Therefore, extension wires were connected to the shield and board headers to minimize the weight of the whole assembly on the riflescope. The extension wires and assembly are pictured in Fig. 1.

Figure 1:
ADXL372 assembled on the riflescope

A more precise image of the sensor assembly and orientation is represented in Figure 2.
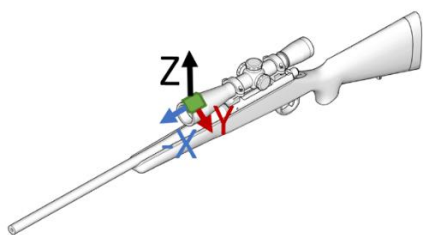

Figure 2:
ADXL 372 position and orientation

3. Results

While reading the sensor data, the ADXL372 post processes the acquired data with a low pass filter to enforce the Nyquist law. The following images will show the acquired accelerometer data over the three axes processed through a low pass filter.

Figure 3 below shows the accelerometer data for the x-axis. It is noticeable that the acquired data contains high frequencies by not having any data points between the peak and the consecutive data point being the local low, as shown in Fig. 3.
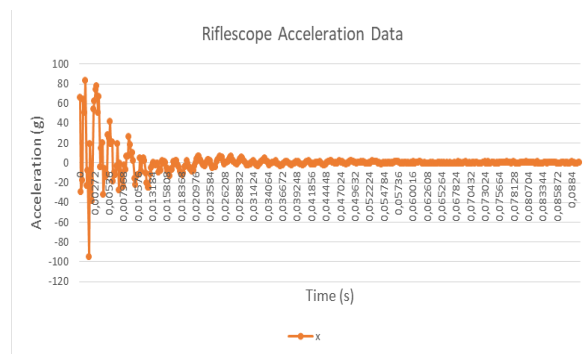

Figure 3:
Riflescope acceleration x-axis

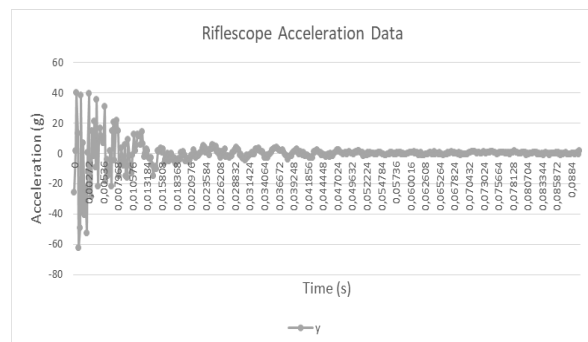Figure 4 shows the y-axis acceleration data similar in behavior to the x-axis data above.

Figure 4:
Riflescope acceleration y-axis

Figure 5 shows the z-axis accelerometer data. Contrary to what was measured for the x and y axes, the z-axis acceleration data clearly shows a well-defined sinusoidal wave attenuating over time and converging to zero. In addition, each half wave is distinctly defined by multiple points, indicating a lower frequency vibration.

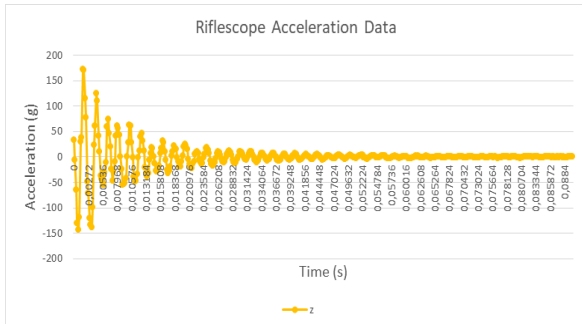Figure 6 shows the velocity magnitude calculated by integrating the accelerometer data for the three axes.

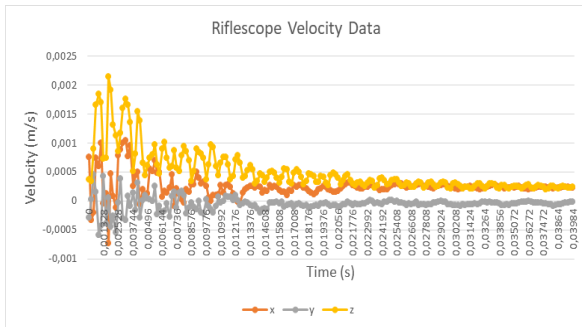**Figure 5:**
Riflescope acceleration z-axis

Figure 6:
Riflescope velocity

Figure 7 shows the displacement calculated from double integrating the accelerometer data for the three axes.
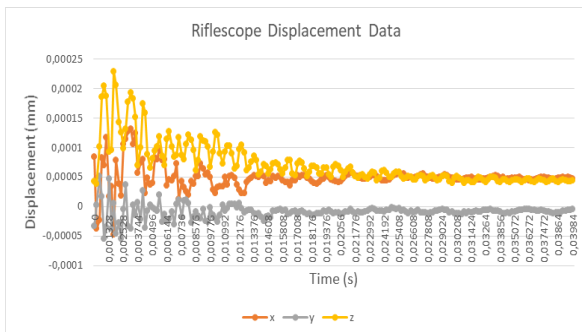

Figure 7:
Riflescope displacement

Figure 8 shows the calculated three-axis displacement in 3D space. The color-code scale is defined as time in seconds, which makes interpreting the data more accessible. This graph represents the riflescope movement in 3d space and shows how it not only vibrates but also shifts locations from the start time (blue) to the end time (red).

Figures 9, 10 and 11 show the calculated FFT data for the x, y, and z axes, respectively. The FFT was calculated in excel using 2^5 data points.
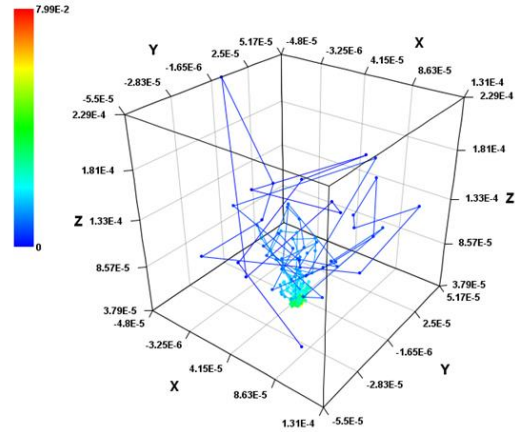

Figure 8:
Riflescope 3D displacement

Figure 9 shows dominant data frequencies at 60Hz, 400 Hz, and 500 Hz on the x-axis. Other higher frequencies are also present in the data, with about half the magnitude of the dominant frequencies. Having such higher frequencies closer to the Nyquist limit implies having jagged or sharp data curves making the data difficult to analyze and interpret.
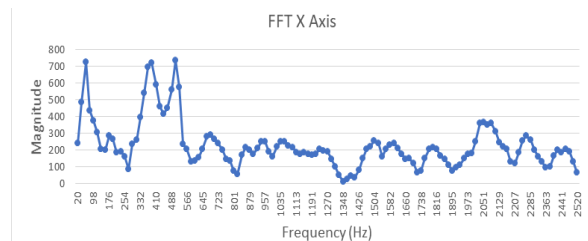

Figure 9:
FFT on the x-axis

Figure 10 shows dominant data frequencies at 260Hz, 1400 Hz, and 2200 Hz in the y-axis. Here the higher frequencies closer to the Nyquist limit are also more dominant and have similar magnitudes to the harmonic frequency. Similarly to the x-axis and even more exaggerated, these frequency magnitudes imply having jagged or sharp data curves making the data difficult to analyze and interpret.
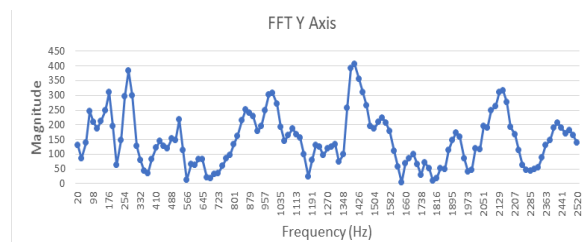

Figure 10:
FFT on the y axis

Figure 11 shows a harmonic frequency at around 500 Hz on the z-axis. Few higher frequencies are present in the data with relevant magnitudes to the harmonic frequency. This harmonic is most relevant when interpreting the post-processed acceleration data in the z-axis. The acceleration data curves are well-defined by multiple points and can be directly used to compare and validate analytical data.
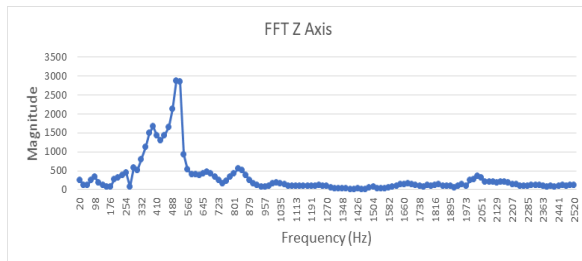

Figure 11:
FFT on the z axis

4. Conclusions

Experimental data is crucial to characterize the riflescope movement during a shot. Therefore, various accelerometers were researched and compared between working principles, specifications, and prices. Based on the selection criteria, the ADXL372 was selected. The shield was connected to the Arduino Mega due to its higher internal memory to save all the necessary data points.

The sensor must be mounted onto the riflescope without interfering too much with the function and recoil wave propagation. Therefore, a 3D support was manufactured, and epoxy was glued onto the riflescope objective using an alignment tool. The support will systematically align the ADXL 372 sensor using two tightly tolerance pins. Thus, making it ideal for easy assembly and testing.

Considering that the acquired accelerometer data has a low pass filter to enforce the Nyquist law, the accelerometer data showed that the maximum recoil on the z-axis is close to the sensor's specified measuring range. The x and y axis are below even the 100 g mark. Also, the z-axis seems to form a clean curve. A periodic sinusoid with multiple data points defining each half sinusoid is depicted in the data. On the other hand, the x and y axis do seem to jump between extremes. One way to make the data more consistent would be to have a low pass filter at

1000 Hz to have multiple data points describing each sinusoid leg.

The acceleration data was once integrated to generate a velocity graph and twice integrated for the displacement graph. Observing the graphs, the z and x axes had a larger movement than the y axes. Also, from the x and z axes dataset, there was vibration and displacement. In other words, there was movement in the x and z axis that once the riflescope came to rest, the accelerometer was no longer at the origin.

The accelerometer data was also used in an FFT analysis. This analysis helped to discover the more dominant frequencies in the dataset and to justify why the acceleration in the z axis is of higher magnitude but more periodic than the x and y axes. The z-axis has a dominant frequency at around 500 Hz, meaning that the sensor picked up on slower-moving frequencies that, in turn, have larger amplitudes. In contrast, the x and y axes have harmonic frequencies present over the entire range meaning more fast-moving waves with smaller amplitudes.

5. Acknowledgements

6. References

[1] M. Liennard, O. Chevalier, A. Langlet, Y. Guilmard, and M. Mansion, (2018)."An analysis of the accelerations of a projectile in a gun tube by direct measurements and telemetry of the data," Mech. Ind., vol. 19, no. 4, p. 406, doi: 10.1051/meca/2018020.

[2] E. Brueck, "Assessment of firearm moderators (short report),"(2004). Accessed: Jan. 05, 2020. [Online]. Available: https://www.hse.gov.uk/research/hsl_pdf/2004/hsl04-01.pdf.

[3] B. Lonzi, M. Martarelli, C. Santolini, and L. Scalise, (2014). "Measurement of firing impulse force in rifles".

[4] "Accelerometers: Piezoelectric, MEMs and Piezoresistive Accelerometers Explained - Latest Open Tech From Seeed." https://www.seeedstudio.com/blog/2020/12/14/accelerometers-piezoelectric-mems-and-piezoresistive-accelerometers-explained/ (accessed Oct. 20, 2022).

[5] E. Spence, (2016) "MEMS Accelerometer Performance Comes of Age".

[6] J. Shieh, J. E. Huber, N. A. Fleck, and M. F. Ashby, "The selection of sensors," Prog. Mater. Sci., vol. 46, no. 3–4, pp. 461–504, Jan. 2001, doi: 10.1016/S0079-6425(00)00011-6.

[7] TE Connectivity, "CHOOSING THE RIGHT TYPE OF ACCELEROMETER," 2017. Accessed: Jun. 02, 2020. [Online]. Available: https://www.mouser.com/pdfdocs/choosing-the-right-accelerometer-white-paper.pdf.

[8] PCB Piezotronics, "Test & Measurement Products," Depew, NY. Accessed: May 22, 2020. [Online]. Available: www.pcb.com.

[9] A. S. Fiorillo, C. D. Critello, and A. S. Pullano, (2018). "Theory, technology and applications of piezoresistive sensors: A review" Sensors Actuators A Phys., vol.281, pp156-175,doi:10.1016/J.SNA.2018.07.006.

[10] J. P. Polizzi, B. Fain, and F. Maspero, "Accelerometer, (2020). Handb. Silicon Based MEMS Mater. Technol., pp.879–898, doi: 10.1016/B978-0-12-817786-0.00045-1.

[11] Y. Shi et al., (2018)."Design, fabrication and calibration of a high-G MEMS accelerometer," Sensors Actuators A Phys., vol. 279, pp. 733–742, doi: 10.1016/J.SNA.2018.07.010.

[12] E. H. Dulf, D. Copot, L. C. Miclea, M. Macias, D. Sierociuk, and W. Malesza, (2022). "MEMS Accelerometer Noises Analysis Based on Triple Estimation Fractional Order Algorithm," Sensors 2022, Vol. 22, Page 527, vol. 22, no. 2, p. 527, Jan. 2022, doi: 10.3390/S22020527.

[13] F. Mohd-Yasin, D. J. Nagel, and C. E. Korman, (2010)."Noise in MEMS," Meas. Sci. Technol., vol. 21, no. 1, 2010, doi: 10.1088/0957-0233/21/1/012001.

[14] K. Group, "Electronics & Software KiDAQ Data Acquisition Modular and flexible DAQ system," 2018. Accessed: May 22, 2020. [Online]. Available: www.kistler.com.

[15] K. Instrument Corp, "Ceramic Shear Triaxial Accelerometer Miniature IEPE Triaxial Accelerometer, with TEDS Option." Accessed: May 22, 2020. [Online]. Available: www.kistler.com.

[16] K. Group, "Electronics & Software KiDAQ Module 5512A Measurement module for IEPE sensors (Piezotron) and voltage," 2018. Accessed: May 22, 2020. [Online]. Available: www.kistler.com.

[17] "SIRIUS Technical Specifications Dewesoft. "https://dewesoft.com/products/daq-systems/sirius/tech-specs (accessed May 22, 2020).

[18] N. Yazdi and K. Najafi, (2000)."Performance limits of a closed-loop, micro-g silicon accelerometer with deposited rigid electrodes," Proc. Int. Conf. Microelectron. ICM, vol. 2000-October, pp. 313–316, doi: 10.1109/ICM.2000.916467.

[19] B. C. Baker, (2004). "ANALOG DESIGN NOTE ADN007 Techniques that Reduce System Noise in ADC Circuits," Microchip Technology Inc.

[20] T. Neu, (2015). "Why your high-speed ADC can never have enough SNR", Nat.Inst, USA.

[21] L. B. Pupo, (2016). "Characterization of Errors and Noises in MEMS Inertial Sensors Using Allan Variance Method," Universitat Politecnica de Catalunya.

[22] F. Levinzon, (2005). "Measurement of low-frequency noise of modern low-noise junction field effect transistor" doi: 10.1109/TIM.2005.858534.

[23] S. Elmer and J. Martin,(2009) "Fourier Series Approximations and Low Pass Filtering, "SportsCience, vol.13 , no. 1–8, Accessed: Oct. 05, 2022. [Online]. Available: https://sportsci.org/2009/sjejcm.htm.

[24] "Noise Measurement | Fierce Electronics." https://www.fierceelectronics.com/embedded/noise-measurement (accessed Oct. 22, 2022).

[25] Wilcoxon Sens, (2020) "Understanding the accelerometer noise specification".

[26] D. S. Arar, (2022). "Accelerometer Specifications: Measurement Range, Sensitivity, and Noise Performance," All about Circuits.

[27] V. J. S. Botero, W. Hernández, and E. Fernández, (2014). "Orientation of a triaxial accelerometer using a homogeneous transformation matrix and Kalman filters," Int. J. Smart Sens. Intell. Syst., vol. 7, no. 4, pp. 1631–1646, doi: 10.21307/ijssis-2017-724.

[28] A. Devices, "ADXL 371 Micropower, 3-Axis, ±200 g Digital Output, MEMS Accelerometer," Accessed: Oct. 19, 2022. [Online]. Available: www.analog.com.

[29] A. Devices, "ADXL372 Data Sheet." Norwood, Aug. 2018, Accessed: Feb. 12, 2022.[Online]. Available: www.analog.com.

[30] A. Devices, "ADXL 375 3-Axis, ±200 g Digital MEMS Accelerometer," Accessed: Oct. 19, 2022. [Online]. Available: www.analog.com.